Supporting information

Construction of AgBr-Ag_2MoO_4 heterojunction and its photocatalytic sterilization activity

1. Weighing potassium bromide 0.0526 g, 0.111 g, 0.25 g, 0.67 g of different quality, adding 2 ml of deionized water to dissolve, dropping to 1 g Ag_2MoO_4 30 ml suspension to obtain 5%, 10%, 20%, 40% AgBr content of AgBr-Ag_2MoO_4. Then, the antibacterial experiment was carried out. From *Figure S1*, it shows that the antibacterial activity of 10% AgBr-Ag_2MoO_4 is the strongest, and it only takes 80 min to inactivate E.coli.

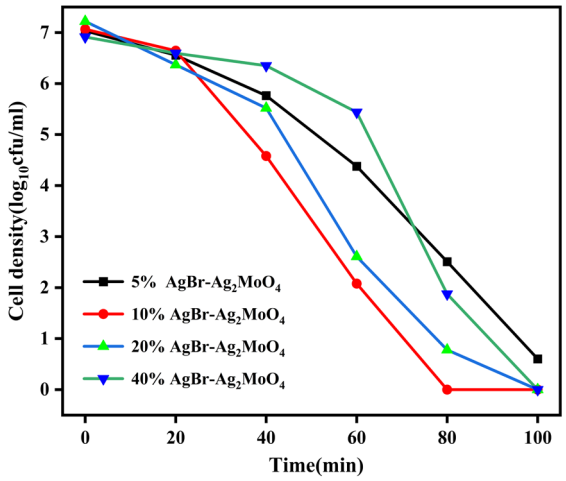

Figure S1. Antibacterial experiment of AgBr-Ag_2MoO_4 with different contents

2. In order to explore whether AgBr-Ag_2MoO_4 has bactericidal effect on different strains, Staphylococcus aureus was used as the template bacteria for the photocatalytic antibacterial experiment. *Figure S2* (a) shows the changes of S.aureus in bacterial concentration in different catalyst systems in dark conditions. In dark conditions, the bacterial concentration decreased very slowly, indicating that these samples show no antibacterial activity in dark. *Figure S2* (b) shows the changes in bacterial concentration in different catalyst systems with light illumination. All S.aureus could be inactivated by adding AgBr-Ag_2MoO_4 within 100 minutes, and the bactericidal effect is slightly weaker than the E. coli.

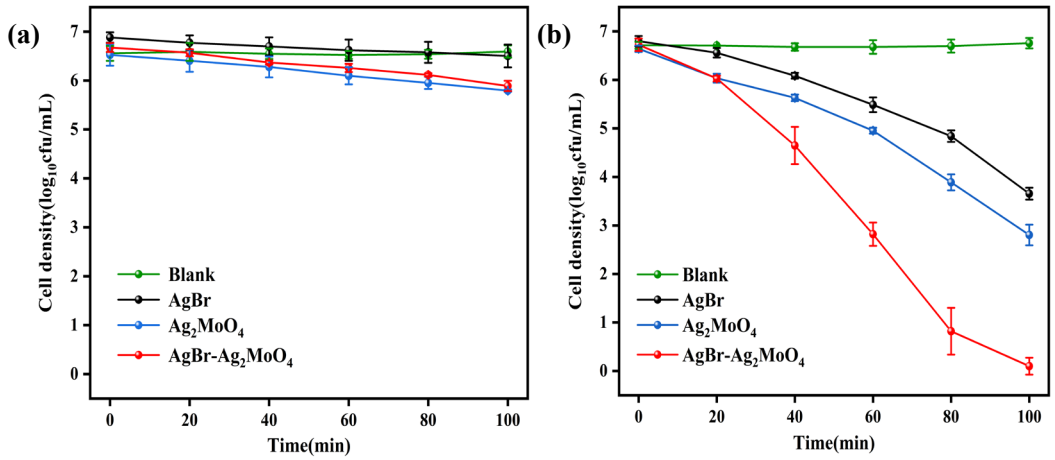

Figure S2. Inactivation of S.aureus by AgBr, Ag_2MoO_4 and AgBr-Ag_2MoO_4 (a) Dark condition and (b) under visible light irradiation

3. The antibacterial stability of catalysts is very important in practical use. Shown in *Figure S3*. The catalyst remaining after each antibacterial experiment was recovered for reuse, and the catalyst was sealed and sterilized at 121℃ for 20 min before the experiment. As shown in *Figure S3*(a), After three successive cycle experiments, it could be observed that the inactivation efficiency of bacteria was still 77% within 100 minutes. At the same time, the sample after repeated experiment was recovered, washed, dried, and subjected to XRD testing. As shown in *Figure S3*(b), all characteristic peaks in the samples still existed. The sample XPS before and after the reaction was shown in *Figure S4*(a-d), and it can be observed that there is no significant change in the constituent elements and the valence states of each element. This further indicates that the composite sample has good stability.

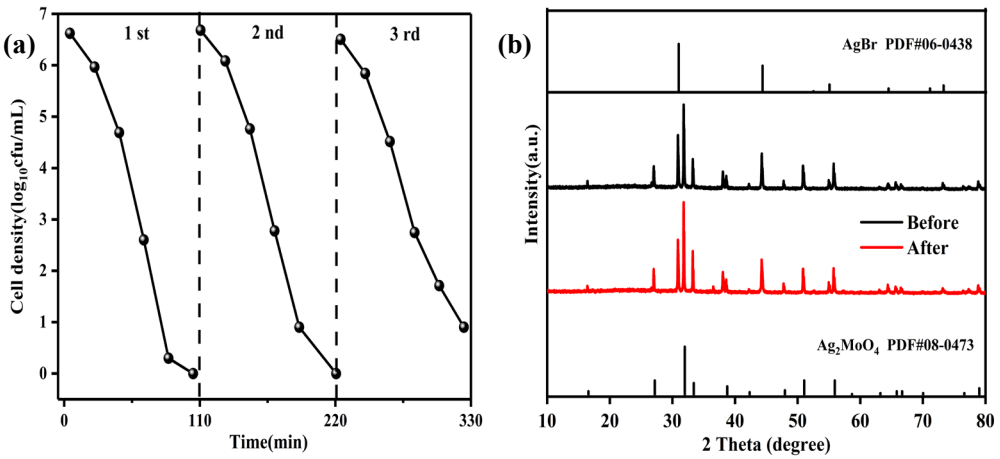

Figure S3. (a)Three cycles of AgBr-Ag_2MoO_4 under visible light, and(b) XRD patterns before and after the reaction

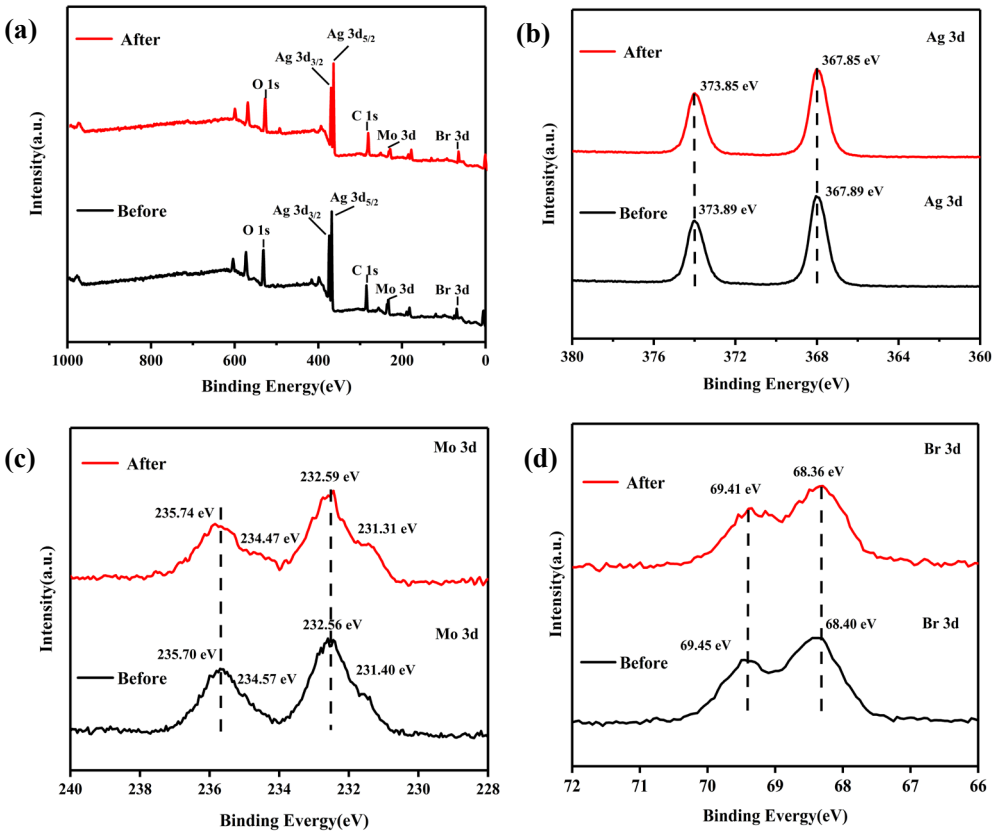

Figure S4. XPS spectra before and after AgBr-Ag_2MoO_4 reaction (a) full spectrum, (b) Ag, (c) Mo, and (d) Br

4. The Ag^+ concentration of catalyst in different periods was measured by ICP-MS to predict the influence of ions on the sterilization process. As shown in *Figure S5*(a), with the increase of reaction time, Ag^+ ionized by AgBr-Ag_2MoO_4 increased gradually at first, and the ion concentration reached a certain equilibrium after 40 min of light exposure,but the effect of precipitated Ag^+ is not obvious under dark conditions. Then, the maximum concentration of Ag^+ about 9.5 mg/L was cconfigured for antibacterial experiments under dark conditions, Shown in *Figure S5*(b). and it was found that the bactericidal effect of Ag^+ was weak.

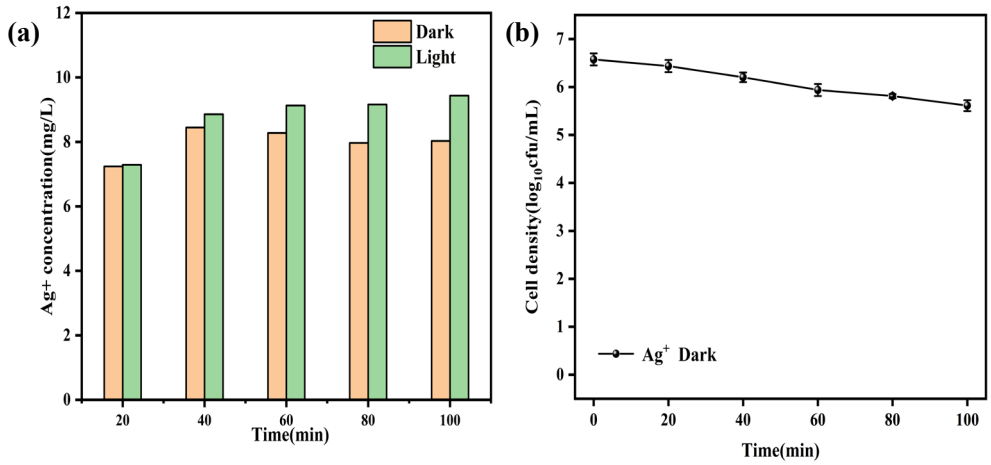

Figure S5. (a) concentrations of AgBr-Ag_2MoO_4 at different reaction time under dark and light conditions, and(b)Inactivation of E.coli of Ag^+ under dark condition

5. 30 mg AgBr and Ag_2MoO_4 were evenly dropped on the monocrystalline silicon wafer, and 800 spots were collected on the surface of both of them in single point mode with Kelvin probe technology to test their surface photovoltage values. Au was used as a reference to compare the work function difference between AgBr and Ag_2MoO_4. The results are shown in *Figure S6.* It can be concluded from the results that the Fermi level of AgBr is higher than that of Ag_2MoO_4. After contact, the electrons of AgBr will flow to Ag_2MoO_4 until the Fermi level reaches the same level, resulting in a corresponding built-in electric field from AgBr to Ag_2MoO_4 is generatedbelow.[1] Under visible light irradiation, the electrons of Ag_2MoO_4 are excited from the valence band to the conduction band, and photogenerated holes are generated in the valence band. Under the action of the internal electric field, the photogenerated e^- on Ag_2MoO_4 (CB) is combined with the photogenerated h^+ on AgBr (VB). At the same time, due to the existence of the Schottky barrier, the migration of electrons from AgBr to Ag_2MoO_4 will be prevented, thereby effectively promoting the separation and transfer of photogenerated e^- and h^+.[2, 3]

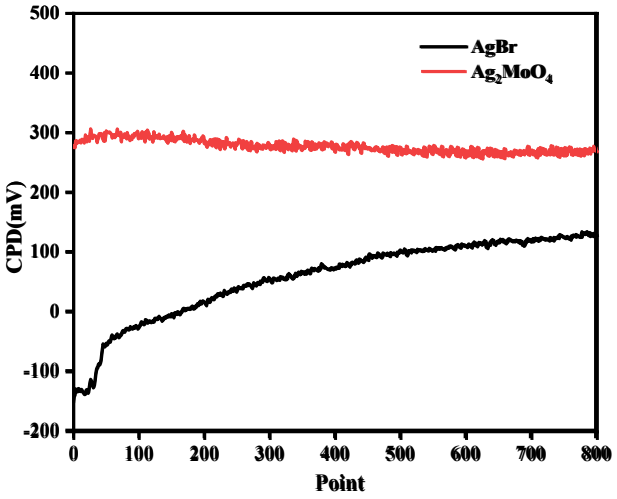

Figure S6. CPDs of AgBr and Ag_2MoO_4 surface related to Au reference at single-point measurement over 1000 points.

6. The conduction band and valence band of the prepared catalyst can be obtained according to the following formula: [4, 5]

$$\alpha h\nu = A(h\nu - Eg)^{n/2}$$

$$E_{VB} = X - E_{CB} + 0.5Eg$$

$$E_{CB} = E_{VB} - Eg$$

Figure S7 (a) is the Mott-Schottky curve of AgBr and (b) is Ag_2MoO_4. It can be seen that the Position of guide belt of AgBr is at -0.53 eV, that is, E_{CB} = -0.53 eV, and the Position of guide belt of Ag_2MoO_4 is 0.88 eV, that is, E_{CB} = 0.88eV. According to the UV-Vis diffuse reflectance spectrum (DRS) data, Band gap of AgBr and Ag_2MoO_4 were obtained with the formula. According to the formula, it can be calculated that the valence band of AgBr is E_{VB}=1.98 eV, and the valence band position of Ag_2MoO_4 is E_{VB}=3.95 eV.

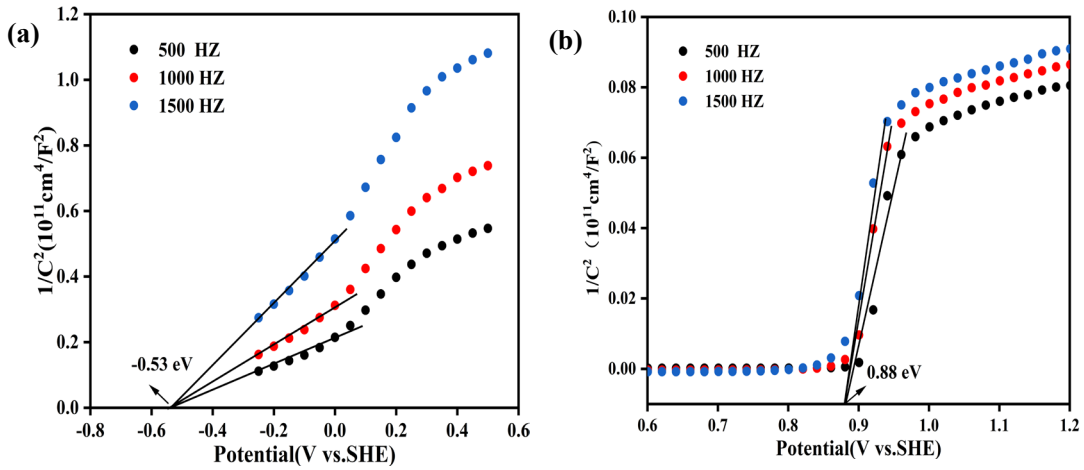

Figure S7. Mott-Schottky curves of (a)AgBr and(b)Ag_2MoO_4

Reference

1. S. Shen, H. Zhang, A. Xu, Y. Zhao, Z. Lin, Z. Wang, W. Zhong and S. Feng, Construction of $NiSe_2/BiVO_4$ Schottky junction derived from work function discrepancy for boosting photocatalytic activity, J. Alloys Compd., 2021, **875**, 160071.
2. S. Ruan, W. Huang, M. Zhao, H. Song and Z. Gao, A Z-scheme mechanism of the novel ZnO/CuO n-n heterojunction for photocatalytic degradation of Acid Orange 7, Mater. Sci. Semicond. Process., 2020, **107**, 104835.
3. J. Jiang, Z. Mu, P. Zhao, H. Wang and Y. Lin, Photogenerated charge behavior of BiOI/g-C_3N_4 photocatalyst in photoreduction of Cr (VI): A novel understanding for high-performance, Mater. Chem. Phys., 2020, **252**, 123194.
4. Z. Wang, K. Dai, C. Liang, J. Zhang and G. Zhu, Facile synthesis of novel butterfly-like Ag_2MoO_4 nanosheets for visible-light driven photocatalysis, Mater. Lett., 2017, **196**, 373-376.
5. Z. Xia, J. Min, S. Zhou, H. Ma, B. Zhang and X. Tang, Photocatalytic performance and antibacterial mechanism of Cu/Ag-molybdate powder material, Ceram. Int., 2021, **47**(9), 12667-12679.